

# High quality factor resonance at room temperature with nanostrings under high tensile stress

Scott S. Verbridge and Jeevak M. Parpia

*Department of Physics, Cornell University, Ithaca, New York 14853*

*and Cornell Center for Materials Research, Cornell University, Ithaca, New York 14853*

Robert B. Reichenbach

*Department of Electrical Engineering, Cornell University, Ithaca, New York 14853*

*and Cornell Center for Materials Research, Cornell University, Ithaca, New York 14853*

Leon M. Bellan and H. G. Craighead<sup>a)</sup>

*School of Applied and Engineering Physics, Cornell University, Ithaca, New York 14853*

*and Cornell Center for Materials Research, Cornell University, Ithaca, New York 14853*

(Received 16 November 2005; accepted 11 April 2006; published online 23 June 2006)

Quality factors as high as 207 000 are demonstrated at room temperature for radio-frequency silicon nitride string resonators with cross sectional dimensions on the scale of 100 nm, made with a nonlithographic technique. A product of quality factor and surface to volume ratio greater than 6000 nm<sup>-1</sup> is presented, the highest yet reported. Doubly clamped nanostring resonators are fabricated in high tensile-stress silicon nitride using a nonlithographic electrospinning process. We fabricate devices with an electron beam process, and demonstrate frequency and quality factor results identical to those obtained with the nonlithographic technique. We also compare high tensile-stress doubly clamped beams with doubly clamped and cantilever resonators made of a lower stress material, as well as cantilever beams made of the high stress material. In all cases, the doubly clamped high stress beams have the highest quality factors. We therefore attribute the high quality factors to high tensile stress. Potential dominant loss mechanisms are discussed, including surface and clamping losses, and thermoelastic dissipation. Some practical advantages offered by these nanostrings for mass sensing are discussed. © 2006 American Institute of Physics.

[DOI: 10.1063/1.2204829]

## I. INTRODUCTION

Resonant mechanical structures with dimensions in the micron to submicron regime offer distinct advantages over their larger mechanical and electrical counterparts in system miniaturization, power conservation, and force sensitivity. These structures have the potential to replace bulky and power hungry mixers, oscillators, and filters in radio-frequency signal processing applications.<sup>1,2</sup> They have been employed to measure mass with sensitivity approaching azeptogram (10<sup>-21</sup> g),<sup>3,4</sup> and have enabled continuous position measurement close to the fundamental limit set by quantum mechanics.<sup>5</sup> In all these applications, the benefits of using micro- or nanoelectromechanical resonators relate directly to small size, high frequency, and spectral purity. This last quantity is defined by the mechanical quality factor  $Q = f_0/\Delta f_0$ , where  $f_0$  is the resonant frequency and  $\Delta f_0$  is the full width at half power of the resonance peak. Increasing quality factor relative to some measure of size can be advantageous for a number of applications of nanoscale resonators. For mass sensing, it is desirable to minimize  $M_{\text{eff}}/Q$ , where  $M_{\text{eff}}$  is effective resonator mass, in order to minimize measurable bound mass.<sup>4</sup> Yasumura *et al.*<sup>6</sup> show that the minimum force detectable with a cantilever resonator is proportional to  $(wt^2/lQ)^{1/2}$ , where  $w$  is resonator width,  $t$  thickness,

and  $l$  length. To the detriment of device performance in many cases, a tendency for  $Q$  to degrade with shrinking device dimensions has been observed.<sup>7,8</sup>

Mechanical quality factors of microscale resonators made from single crystal silicon have been elevated into the range of tens and even hundreds of thousands by high temperature annealing<sup>6,9–11</sup> and chemical surface treatments.<sup>12</sup> These treatments are thought to help reduce surface-related losses associated with increasing surface to volume. These types of devices have yielded quality factors above 10<sup>6</sup> at low temperatures.<sup>9</sup> Quality factors of nanoscale oscillators made of materials including single crystal silicon, silicon nitride, and silicon carbide are often on the order of thousands.<sup>7,13,14</sup> Materials and processes for nanoscale resonators with quality factors in the range of tens of thousands and above are of particular interest.

## II. NONLITHOGRAPHICALLY DEFINED DEVICES

We demonstrate nanoscale string-type resonators with quality factors exceeding 10<sup>5</sup>, fabricated from a material that can be deposited with low pressure chemical vapor deposition (LPCVD) like many materials already used for nanomechanical structures. Fabrication requires only low resolution photolithography tools. The resonators were fabricated using a process that involves electrospinning poly(methyl methacrylate) (PMMA) nanofiber masks, aligned with photolithographically defined support structures.<sup>15</sup> Devices were made

<sup>a)</sup>Electronic mail: hgc1@cornell.edu

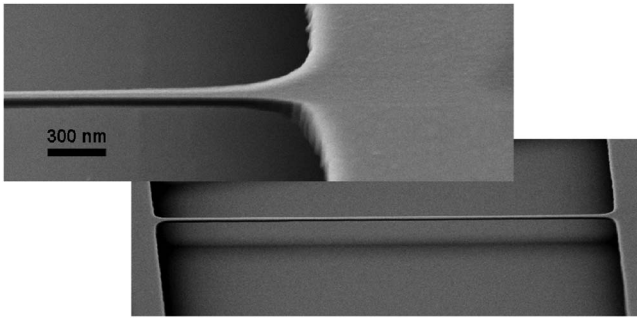


FIG. 1. SEM images of a 15  $\mu\text{m}$  long silicon nitride nanostring, with thickness of 120 nm, and width less than 200 nm. A 300 nm scale bar is shown.

from a high tensile stress ( $1200 \pm 50$  MPa, measured with a wafer bow technique) LPCVD silicon nitride, deposited on silicon dioxide. After fabrication, devices were mounted on a piezoelectric buzzer for resonant actuation, placed in a room temperature vacuum chamber, and pumped down to a pressure below  $10^{-6}$  Torr. The high vacuum eliminates viscous damping effects on string resonance. Figure 1 shows scanning electron micrographs of a silicon nitride string with thickness of 120 nm, width less than 200 nm, and length of 15  $\mu\text{m}$ .

### III. CHARACTERIZATION

Resonances of silicon nitride strings with thicknesses near 100 nm and widths ranging from 100 to 700 nm defined by electrospun masks were measured with an optical detection technique similar to that described in the literature.<sup>3,15</sup> To determine the dependence of resonance parameters  $f_0$  and  $Q$  on string geometry, we employed a scanning electron microscope (SEM) to determine the dimensions of a number of strings of different resonant frequencies and quality factors. The results from such measurements on strings made from the same 120 nm thick silicon nitride film are shown in Fig. 2. Each point represents a measurement made on a single string, with multiple representative strings measured for each principle size range. Resonant frequency was found to vary as the inverse of the length [Fig. 2(a)], hence the term “string” instead of “beam” used in reference to these structures. From standard beam theory,<sup>16</sup> the resonant frequencies of a doubly clamped beam of arbitrary tensile force  $S$  (assuming for simplicity that the ends are simply supported) are given by

$$f_i = \frac{i^2 \pi}{2l} \sqrt{\frac{EI}{\rho A}} \sqrt{1 + \frac{Sl^2}{i^2 EI \pi^2}}, \quad (1)$$

where  $i$  is an integer mode index, and  $l$ ,  $E$ ,  $I$ ,  $\rho$ , and  $A$  are length, Young’s modulus, cross sectional inertia, density, and cross sectional area, respectively. In the limit of low stress, this yields the familiar beam frequency dependence on the inverse of length squared [the mode index for beam frequency in the case of fixed ends is not really an integer index, and must be solved for numerically, yielding an index closer to  $i+(1/2)$ ]. In the limit of high stress we find

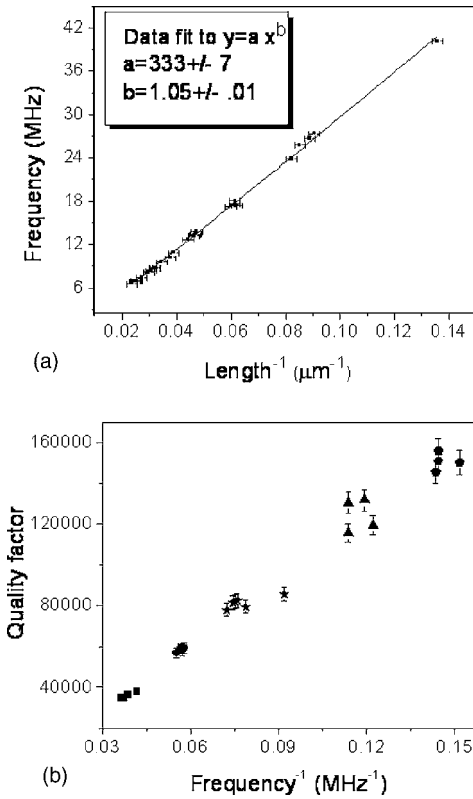


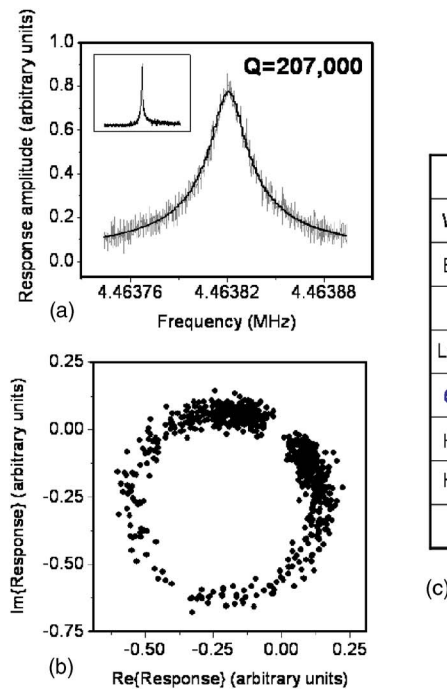
FIG. 2. (a) Length dependence of frequency, with a linear fit, demonstrating the approximate  $1/l$  stretched string equation for resonant frequency  $f_0$ . (b) Quality factor as a function of inverse frequency, for several sets of strings, with similar frequencies within a given set. These symbol coded sets, from low to high quality factor, correspond to length ranges of 11–13, 16–17, 21–26, 31–34, and 40–43  $\mu\text{m}$ .

$$f_i = \frac{i}{2l} \sqrt{\frac{S}{\rho A}}, \quad (2)$$

which is simply the equation for the frequencies of a stretched string, with tensile force  $S$ , and linear density  $\rho A$ . Thus the frequency-length relationship of our structures has been tailored through the choice of a high stress film. From the fit shown in Fig. 2(a) and an assumed silicon nitride density of 3180 kg/m<sup>3</sup> (theoretical value given in Pierson<sup>17</sup>) a string tensile stress ( $S/A$ ) of  $1410 \pm 60$  MPa can be calculated. This value is slightly greater than the tensile stress measured in the film with the wafer bow technique, probably indicating that we are achieving a density less than the theoretical value assumed. A density of 2700 kg/m<sup>3</sup>, closer to that measured for lower stress LPCVD silicon nitrides,<sup>18</sup> would be consistent with the measured tensile stress of 1200 MPa.

Quality factor was found to scale with inverse frequency, as shown in Fig. 2(b), and therefore also with length. It is worth noting that the 40 MHz resonance point included in Fig. 2(a) is not present in (b). This is due to the poor signal-to-noise ratio attained for this resonance, resulting from the exceedingly low response of the piezoactuator at such a high frequency. The measured signal was sufficient to allow for a determination of resonant frequency, but prevented an acceptable Lorentzian fit for quality factor determination.

In Figs. 3(a) and 3(b) we show the optically measured



response (amplitude of the ac component of the reflected detection laser light) of a 200 nm wide, 105 nm thick, 60  $\mu\text{m}$  long electrospun fiber defined string, representing the longest string we were able to make without critical point drying during processing. The quality factor was determined by fitting the amplitude to a Lorentzian curve, yielding  $Q = 207\,000(\pm 10\,000)$ . Variation of detection laser power, as well as changes ( $\times 2$ ) in drive amplitude, did not alter the resulting response shape, confirming that the response measured is within the linear regime. The circularity of the phase plot shown in Fig. 3(b) also indicates that the measured resonance is within the linear regime.

In Fig. 3(c), we compare our highest quality factor with others from the literature, obtained with flexural beam resonators with similar surface to volume ratio  $R$ . We include data from Wago *et al.*<sup>19</sup> to point out the larger dimensions typically required to achieve quality factors exceeding  $10^5$ . Included are data that represent the highest quality factors we have found in the literature for resonators at this size scale, specifically with cross section less than a micron. It should be pointed out that many of the referenced devices required a metal layer as part of the drive and detection schemes, potentially resulting in a diminished quality factor. One advantage of our drive and detection scheme is that it requires no metal layer, and hence avoids any potential dissipation resulting from the metal coating. We note that our resonators have the highest  $Q$  (207 000) as well as the highest  $RQ$  product ( $6013 \text{ nm}^{-1}$ ) of any flexural resonator among the devices considered.  $RQ$  is a measure of quality factor normalized to surface to volume ratio. Liu *et al.* pointed out this interpretation of  $RQ$  as a measure of oscillator performance, due to the observed tendency of  $Q$  to decrease with increasing  $R$ .<sup>20</sup> It is interesting to note that the points displayed here represent the highest values obtained at any temperature, and many of the data points from other resonators were taken at low temperature, where the intrinsic  $Q$  is expected to be enhanced.

FIG. 3. (Color online) (a) Amplitude of the ac component of a continuous wave laser beam reflected from the vibrating string with a Lorentzian fit giving a quality factor of 207 000. The magnified peak corresponds to a 150 Hz span, and the small inset to 1.5 kHz. (b) Imaginary vs real part of the phase information from the response displayed in (a). (c) Comparison of our results with results from the work of others on flexural resonators with similar surface to volume ratios. This table refers to Refs. 3, 5, 14, 19, and 32–34. Dimensions given are cross sectional dimensions, and  $R$  is surface to volume ratio.

The highest quality factors we demonstrate result from our highest aspect ratio devices, with large ratios of length to other critical device dimensions. A clear comparison with devices which are similar in both cross section and length is necessary to emphasize the different quality factors observed for the high stress devices presented. We compare our devices with those fabricated by Sekaric *et al.*<sup>13</sup> in a low stress, silicon-rich LPCVD silicon nitride (172 MPa tensile). In this previous work, doubly clamped beams were fabricated using electron beam (e-beam) lithography, yielding quality factors of less than 5000 for 8  $\mu\text{m}$  long structures, with width and thickness on the order of hundreds of nanometers. If it is assumed that the trends shown in Fig. 2 continue to shorter structures, an extrapolation for 8  $\mu\text{m}$  long strings made from high stress nitride yields a quality factor of 27 000, representing a fivefold increase for devices differing only in material details and fabrication steps. The source of the increased quality factors demonstrated will be considered in the following.

#### IV. SURFACE LOSSES AND FABRICATION INDUCED DAMAGE

It has been suggested that quality factor for resonators in the size range we are considering can be strongly dependent on surface to volume ratio. For instance, in Ref. 7, the quality factor was observed to decrease almost linearly with increasing surface to volume, over a range of surface to volume that includes the range considered in our work. The devices used for this study, however, were metallized, and it is unclear to what extent this metallization influenced the dissipation in these measurements. Furthermore, quality factors in this work did not exceed 3000, significantly lower than the quality factors we are observing in our high stress devices, indicating that dominant sources of dissipation should be expected to differ between these two sets of devices. Quality factors decreasing linearly with increasing sur-

face to volume have also been observed in larger micromechanical resonators, made of amorphous silicon,<sup>21</sup> but again it is not clear that the dissipation in this case is not due in some part to surface contamination resulting from specific processing steps.

It has been observed that improvements in quality factor of mechanical resonators can be achieved by chemical surface treatments,<sup>12</sup> as well as annealing steps<sup>11</sup> thought to result in deoxidation of the surface of silicon resonators. It is not obvious, however, how important surface oxides would be in the case of a resonator made from materials other than pure silicon. Nanoscale resonators made from a variety of materials including low stress silicon nitride,<sup>13</sup> silicon carbide,<sup>22</sup> and diamond<sup>23</sup> have exhibited lower quality factors at room temperature than we have achieved with high stress silicon nitride, with surfaces which at the very least would not oxidize in the same way as a silicon surface.

As a result of our measurements on high tensile-stress nanostrings, we find that strings with the same frequency do not exhibit a significant quality factor difference with varying surface to volume over the range explored. For example, we consider the pair of strings measured with lengths of 21.57 and 21.09  $\mu\text{m}$ , and widths 606 and 154 nm. These strings exhibit almost a factor of 4 difference in width, corresponding to surface to volume ratios differing by about 50%, while their frequencies (13.16 and 13.82) and quality factors (82 500 and 78 100) only differ by about 5%. On the other hand, we consider a pair of strings with identical thickness (120 nm) and similar widths (269 and 275 nm), hence similar surface to volume ratios. These beams differ in length (11.04 and 40.60  $\mu\text{m}$ ), resulting in frequencies (27.36 and 6.93 MHz) and quality factors (34 700 and 151 000) differing by about a factor of 4. It is therefore clear that quality factor variation is not determined by surface to volume ratio in the range explored, as significant variations in  $Q$  are evident with similar surface to volume, while similar  $Q$ 's are evident for varied surface to volume, and in all cases the quality factor was observed to depend inversely on frequency. We therefore exclude surface losses as a likely dominant source of dissipation in our resonators.

Another possible loss mechanism that should be considered, perhaps related to surface losses in some cases, would be losses due to fabrication induced damage. We have compared our high stress resonators with resonators made by Sekaric *et al.*, which were made with electron beam lithography. There exists the possibility that different fabrication procedures might be the source of our unexpectedly high quality factors. We tested the potential impact of fabrication steps on the mechanical quality factor by comparing three sets of nearly identical devices, resulting from three different fabrication processes: nanostrings fabricated using electrospun PMMA nanofiber masks, similar devices that were coated with 30 nm Cr which was removed before release, and nanostrings fabricated with electron beam lithography (100 keV exposure of FOX-16 resist). All three sets were fabricated from the same substrate, and released in the same step, to test both the effects on quality factor of the e-beam exposure itself as well as any Cr residue that might result from a Cr hard mask, commonly used in e-beam processing.

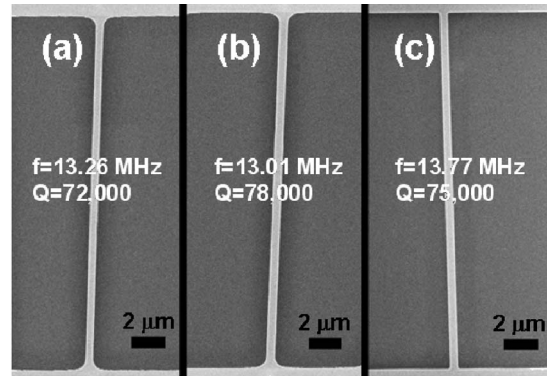


FIG. 4. [(a)–(c)]. SEM images of similar strings made from different processes, with polymer fiber defined strings in (a) and (b) and an e-beam defined string in (c). Scale bars of 2  $\mu\text{m}$  are shown for each string.

In Fig. 4 we show similar strings from each of these sets, with electrospun polymer fiber defined strings in Figs. 4(a) and 4(b), and an e-beam defined string in Fig. 4(c), all with width  $\sim$ 450 nm, 120 nm thickness, and  $\sim$ 20  $\mu\text{m}$  length, all made from our high stress nitride. No significant differences in frequency or quality factor were observed among these sets. We therefore believe that our high quality factors are not a result of fabrication, but rather of the inherent material properties of the resonators.

## V. FURTHER COMPARISONS OF DIFFERENTLY STRESSED DEVICES

Our own experiments comparing resonators made of differently stressed silicon nitrides verify that the higher stress devices have the highest quality factors for a wide range of frequencies. Comparisons were made of the quality factors of doubly clamped beams made with 105 nm thick high stress nitride and 220 nm thick low stress nitride (tensile stress  $\sim$ 200 MPa). The devices compared were chosen to have similar resonant frequencies (47 and 48 MHz), similar widths (200–400 nm from electrospun masks), and similar lengths (6.6 and 5.6  $\mu\text{m}$ ). An optical excitation technique identical to that reported by Illic *et al.*<sup>24</sup> was used to excite these frequencies which would have been difficult to access with piezoactuation. These devices were released in the same process step, assuring the same undercut details. The high stress resonator demonstrated a quality factor approximately a factor of 3 higher than the low stress resonator (17 000 5000). It should be pointed out that the low stress nitride device mentioned here was made from a thicker substrate than the high stress device. This was convenient in that it allowed two devices to be compared with nearly the same frequency and size. Low stress nitride resonators were also made from 115 nm thick films, with measured quality factors that were slightly less than those from the thicker film. A 5.4  $\mu\text{m}$  long, 115 nm thick low stress beam, for example, had a frequency of about 21 MHz, and a quality factor of less than 3000.

Up to this point, devices of similar geometries but with different material composition have been compared. A difference in quality factor between high and low stress nitride resonators has been observed, with the list of factors possibly

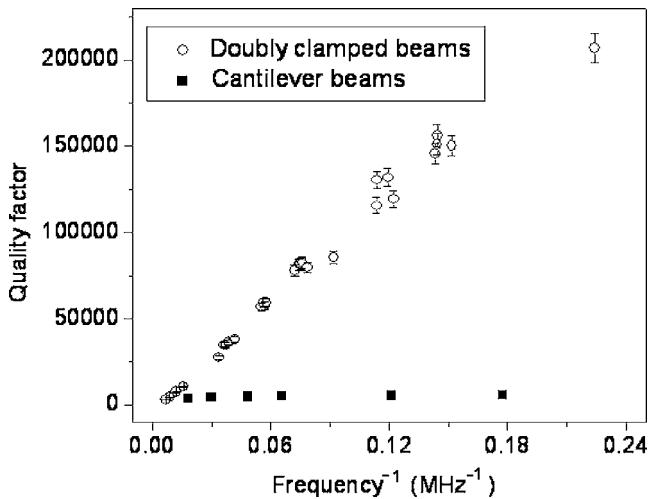


FIG. 5. Quality factor as a function of inverse frequency, for an extended frequency range from that shown in Fig. 2, with data from both doubly clamped beams and singly clamped cantilevers made from the high stress silicon nitride.

influencing this difference narrowed down to the differences between these two materials. The high stress film has a measured stress of 1200 MPa and an index of refraction of 2. The low stress film has a measured stress closer to 200 MPa and an index of refraction of 2.2. Therefore these materials differ both in their stress states and their chemical composition, specifically the lower stress material has a higher silicon content. We eliminate chemical composition as a likely determining factor by considering a carefully fabricated set of resonators made only from a high stress silicon nitride film. This set is composed of both doubly clamped and singly clamped cantilever resonators, all 750 nm wide and 105 nm thick, made photolithographically. Resonators of these two types were examined. Laser actuation was employed to extend the range of accessible frequencies beyond that demonstrated in Fig. 2. Singly clamped cantilevers with lengths between 1.6 and 5.4  $\mu\text{m}$ , and resonant frequencies from 5 to 55 MHz were examined. We also examined doubly clamped beams of shorter lengths, and hence higher frequencies than those shown in Fig. 2, to compare with the cantilevers on the same chip, as well as determine if the doubly clamped beam quality factor dependence on  $1/f$  continues to hold for lengths down to the scale of the lengths of the cantilevers examined.

Figure 5 demonstrates the dependence of quality factor on  $1/f$  for both doubly clamped and cantilever beams. In the doubly clamped case, we include measurements already displayed in Fig. 2(b) from 120 nm thick devices made from electrospun masks, as well as our measurements from 105 nm thick devices which extend the frequency range in both directions (the higher frequency doubly clamped beams, as well as the cantilever beams were photolithographically defined to be 750 nm wide. This width is at the edge of the range over which quality factor was earlier demonstrated not to depend on width for the nonlithographically defined doubly clamped beams). The new data points from the photolithographically defined devices represent an average of many measurements on multiple nominally identical beams,

as lithographically defined. It should be pointed out that doubly clamped beam frequency continues to be proportional to  $1/f$  over the entire frequency range examined in our experiments. It is also interesting to note that there is little to no observed dependence of the cantilever quality factors on frequency, over a frequency range in which significant quality factor variation is clear in the doubly clamped case. Cantilever quality factors ranged between 4000 and 6000 over the cantilever frequency range examined (5–55 MHz), while doubly clamped beam quality factors ranged from 10 000 to more than 100 000 over the same frequency range, with doubly clamped beam quality factors only falling below cantilever values for doubly clamped beam frequencies above 100 MHz. This finding points to the high tensile stress present in the doubly clamped geometry but not in the cantilever geometry, as the principal reason for the high quality factors exhibited by the nanostrings. The different dependencies of quality factor on frequency also point to qualitatively different dominant damping mechanisms for the two types of resonator.

## VI. CLAMPING LOSSES

Several recent studies have examined the dependence of clamping loss limited quality factors on beam geometry. Most recently, Photiadis and Judge<sup>25</sup> have considered the case most applicable to nanoscale resonators, for which resonator width can be assumed small in comparison with the wavelength of propagating elastic waves in the supporting medium. For a resonant frequency of 100 MHz, and a typical elastic wave speed of 5000 m/s for silicon,<sup>25</sup> we would have an elastic wavelength in the supporting silicon of 50  $\mu\text{m}$ , large compared to any resonator width we are considering, so the assumption of small resonator width seems applicable here. In the case in which the support can be thought of as a thin membrane, with support thickness much less than the elastic wavelength in the base, with support and device thickness equal, it was predicted that

$$Q \propto \frac{l}{w}, \quad (3)$$

where  $l$  is beam length and  $w$  is beam width. In the case in which the support can be thought of as semi-infinite, i.e., the support thickness is large compared to the elastic wavelength in the base, they predicted that

$$Q \propto \frac{l}{w} \left( \frac{l}{t} \right)^4, \quad (4)$$

where  $t$  is resonator thickness. The semi-infinite support model yields quality factors orders of magnitude higher than we are observing, at least  $10^6$ , over the entire size range we have examined. In addition a much stronger dependence on length ( $l^5$ ) than the linear dependence we observe is predicted by this model. The thin membrane support does yield the linear dependence on length that we observe, but also predicts a dependence on inverse width. It has already been mentioned that high stress doubly clamped beams with lengths near 20  $\mu\text{m}$ , and with widths differing by a factor of 4, exhibit quality factors that differ by less than 5%, and this

independence of quality factor on width continues down to even the shortest doubly clamped beams measured. Hence the thin membrane support equation is also incompatible with our observations.

In reality, our case is that of a thin support which extends in length about as far as the gap height underneath the beams, due to the isotropic nature of the wet release step. This thin membrane then couples to a thick slab consisting of sacrificial oxide, over a silicon wafer. Hence our devices fall somewhere in between the two clamping loss extremes considered by Photiadis and Judge. Therefore a more careful treatment, which considers the finite lateral extent of our thin membrane support, might yield a mechanism by which clamping losses can be affected by device stress. A model which takes into account the different force and torque exerted on the supporting membrane due to the high tensile stress present in the string resonator might also relate clamping losses to device stress.

In our comparisons of high stress resonators to low stress resonators, interesting differences became apparent, apart from the higher quality factors exhibited by the high stress devices. It has been mentioned that for devices of the same size made from a high stress film, doubly clamped beams have higher quality factors than cantilevers all the way down to lengths of about 2  $\mu\text{m}$ , with doubly clamped beam quality factor depending strongly on length over the entire examined range. In our measurements on low stress nitride beams, it was noticed that over the range of lengths examined (3–10  $\mu\text{m}$ ), quality factors of both singly and doubly clamped resonators remained constant, at about 5000 and 2500, respectively. Hence in the case of devices made from a low stress film, cantilevers exhibited quality factors that were about twice those of the doubly clamped beams. This is consistent with observations made by Ilic *et al.*,<sup>3</sup> as well as Huang *et al.*,<sup>14</sup> and is consistent with the idea that quality factors in the case of low stress doubly clamped beams and cantilever beams, of the geometry shown here are, in fact, limited strongly by clamping losses. The cantilever beam, with only one clamping point, has twice the quality factor of a doubly clamped beam of the same size, with two clamping points. This is only circumstantial evidence, of course, and its theoretical underpinnings need to be explored with an improved model of clamping losses. A decrease in thickness of a factor of 2 was not observed to increase the quality factor for the doubly clamped low stress beams, and changes in width of a factor of four did not change quality factor significantly for the cantilevers made from a high stress film, hence the clamping loss models previously discussed do not seem to accurately describe the losses that dominate these lower quality factor devices.

## VII. DISCUSSION OF INTERNAL DAMPING MECHANISMS

Internal damping mechanisms include effects such as phonon-electron scattering, phonon relaxation dissipation, and thermoelastic damping. Since silicon nitride is an insulator, we discount phonon-electron scattering as a potentially important loss mechanism. We also ignore phonon-relaxation

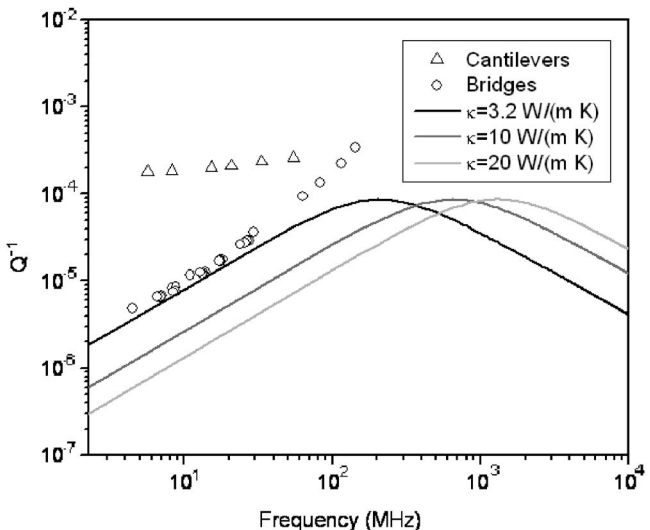


FIG. 6. Quality factor data for doubly clamped beams and cantilevers made from the high stress silicon nitride, plotted with the behavior that would be expected for quality factors limited by thermoelastic dissipation, for three values of thermal conductivity.

dissipation, also sometimes called phonon-phonon scattering, since this would be expected to yield quality factors higher than thermoelastic damping at the size scale we are considering,<sup>26</sup> although it has been suggested that this damping mechanism could become more important than thermoelastic dissipation at size scales below 50 nm.<sup>27</sup> In the present work, we will therefore only consider thermoelastic damping as a potentially observable internal damping mechanism. Thermoelastic damping accounts for the energy dissipation associated with thermal losses resulting from the stretching and compression of portions of a resonator during oscillation. In Fig. 6, we plot inverse quality factor as a function of frequency for both our high stress string and singly clamped cantilever resonators. On this same plot, we also show the quality factor that should be observed in the case in which thermoelastic damping is the dominant dissipation mechanism, using the equation<sup>26,28</sup>

$$Q_{\text{TED}} = \frac{c_v}{E\alpha^2 T} \left( \frac{6}{\xi^2} - \frac{6 \sinh \xi + \sin \xi}{\xi^3 \cosh \xi + \cos \xi} \right)^{-1}, \quad (5)$$

with

$$\xi = t \sqrt{\frac{\omega \rho c}{2\kappa}}, \quad (6)$$

where  $c_v$  is specific heat per unit volume,  $E$  is Young's modulus,  $\alpha$  is the coefficient of linear expansion,  $t$  is resonator thickness,  $\rho$  is density,  $c$  is specific heat per unit mass, and  $\kappa$  is thermal conductivity. We use our measured density of 2700 kg/m<sup>3</sup> and Young's modulus of 211 GPa, calculated from this measured density and our high stress cantilever resonator data. We use an average device thickness of 112.5 nm, and take temperature to be 300 K. For the thermal constants, we use a linear expansion coefficient of  $2.3 \times 10^{-6} \text{ K}^{-1}$  from Chuang *et al.*,<sup>29</sup> for LPCVD nitride, a specific heat per unit volume of 710.6 J/(K m<sup>3</sup>) for bulk nitride,<sup>30</sup> and three thermal conductivity values of 3.2, and

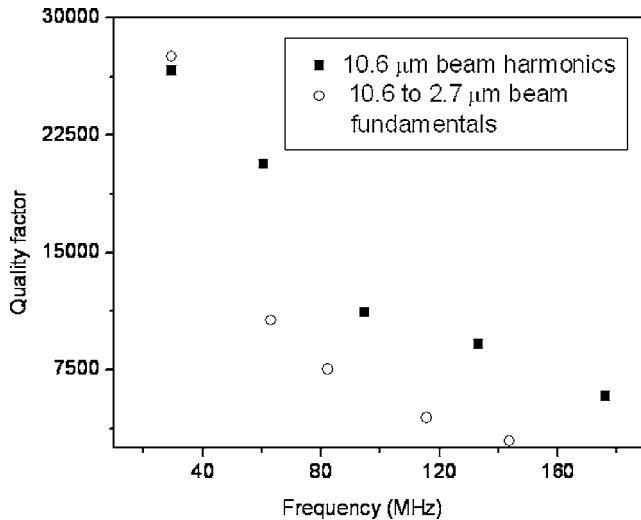


FIG. 7. A comparison of quality factor falloff with frequency for the higher frequency fundamentals vs harmonics.

10 W/(m K), reported by Yasumura *et al.*<sup>6</sup> and Zhang and Grigoropoulos,<sup>31</sup> respectively, for LPCVD films, and 20 W/(m K), typical of values reported for bulk silicon nitride.<sup>30</sup> For the reported LPCVD nitride thermal conductivity values we see that up to a frequency of about 50 MHz, the measured data for the high stress doubly clamped resonators follow the trend given by the thermoelastic dissipation limit fairly well, with an offset in  $Q^{-1}$  of less than an order of magnitude. The fit becomes almost perfect at the lower frequencies for the lower thermal conductivity of 3.2 W/(m K). For the higher conductivity value, the trend is still correct, but the offset is larger. For higher frequency (shorter) resonators, measured quality factors decrease at a rate faster than that predicted by the thermoelastic limit. Figure 6 therefore suggests that variation in quality factor may be related to thermoelastic dissipation, with this dissipation mechanism becoming less evident for higher frequency, and hence shorter resonators. Interestingly, as frequency increases due to decreasing length it is likely that the clamping loss models previously discussed might be expected to become more relevant, due to decreasing length-to-width ratios.

So far only motion at fundamental frequencies has been discussed. We should mention that the falloff seen in quality factor at higher frequencies is not as significant when the damping at harmonics of a beam of a given size are examined, rather than comparison of fundamental modes for successively shorter beams. This trend is shown in Fig. 7, in which we plot the quality factors for fundamental resonances of beams with lengths from 10.6 to 2.7  $\mu\text{m}$ , as well as harmonics from a 10.6  $\mu\text{m}$  beam. This finding is consistent with the notion that quality factor at these higher frequencies is falling off from some combination of thermoelastic as well as clamping-related dissipation, with the length dependent clamping losses becoming more dominant as length is reduced.

### VIII. FURTHER PRACTICAL ADVANTAGES OF HIGH STRESS NANOSTRINGS

High tensile-stress silicon nitride nanostrings offer practical benefits beyond elevated quality factors for their size.

These nanostrings are extremely robust mechanically. These resonant devices with nanoscale cross sections and lengths up to 60  $\mu\text{m}$  have been made without critical point drying. Devices of this scale can be immersed in biomolecule containing buffers, rinsed, and nitrogen dried without succumbing to stiction or breaking. This makes these nanostrings particularly useful for biological sensing in which mass loading must be performed in a fluid environment, while resonance detection is performed in vacuum for maximum quality factor. Nanostrings offer the advantage of high quality factors at room temperature, which is desirable compared to having a requirement of cooling to low temperatures for maximum sensitivity. Finally, we have demonstrated optical interrogation of high quality factor nanostrings. This optical scheme is attractive for sensor systems that are built of a large number of parallel devices. This parallel scheme would increase molecule capture probability in biosensing applications at low sample concentrations, while allowing for individual sensor elements to be addressed without any necessary scaling in the complexity of required on-chip electronics, as would be required with other measurement schemes, such as capacitive, magnetomotive, or piezoresistive detection. This optical detection scheme is also attractive as it does not require the presence of a conducting metal film, which could lead to diminished quality factor.

### IX. CONCLUSIONS

We have presented the fabrication and operation of flexural string resonators with cross sectional dimensions on the scale of 100 nm, and quality factors exceeding  $10^5$  at room temperature. We report the highest  $RQ$  value to date, which can be taken as one measure of the performance of a nanomechanical resonator. We fabricated these high quality factor structures with a nonlithographic technique, using electrospun polymer nanofiber masks. We have demonstrated that the resulting nonlithographically defined structures have mechanical properties that are identical to their counterparts made on the same substrate with electron beam lithography. We have fabricated doubly clamped devices of both high and low stress nitride, and demonstrated that for equal frequencies or equal size, the high stress devices have higher quality factors. Similarly, we have photolithographically fabricated singly clamped resonators from both the high stress and low stress material, and again found that for equal frequencies or length the high stress doubly clamped resonators have the highest  $Q$ , indicating that the stress state is responsible for the unexpectedly high quality factors observed. We show that the trend in quality factors observed for the lower frequency high stress string resonators follows that predicted assuming thermoelastic dissipation, with absolute quality factors within an order of magnitude of this thermoelastic limit. At higher frequencies, quality factors deviate from this thermoelastic trend, possibly due to the increased importance of clamping losses for the shorter devices. The influence of high film stress on resonant frequency and quality factor has thus been demonstrated, and quality factors up to 207 000 have been achieved with nanostrings made from a high stress material. High stress nanostrings offer high quality factors at

room temperature, from devices that are robust enough for immersion in fluids followed by nitrogen drying, making nanostrings promising candidates for biosensing applications.

## ACKNOWLEDGMENTS

The authors would like to thank David Czaplewski, Rob Ilic, Keith Aubin, Lidija Sekaric, and David Tannenbaum for fabrication assistance, helpful discussions of nanomechanical structures, and equipment assistance, Andrew Fefferman and Dmitri Zmeev for verifying our Lorentzian fits for the higher  $Q$  resonators, and Alan Zehnder and Manoj Pandey for helpful discussions of clamping losses and thermoelastic dissipation in nanomechanical resonators. Three of the authors (S.V., L.B., and R.R.) thankfully acknowledge GAANN fellowships and support from the Cornell Center for Materials Research through NSF MRSEC Grant Nos. DMR-0079992 and DMR-0313941. The lithography was performed and the thin films were deposited and characterized at the Cornell Nano-Scale Science and Technology Facility. This research made use of the Cornell Center for Materials Research Shared Experimental Facilities supported through the NSF MRSEC program.

- <sup>1</sup>C. T. Nguyen, L. P. B. Katehi, and G. M. Rebeiz, Proc. IEEE **86**, 1756 (1998).
- <sup>2</sup>R. B. Reichenbach, M. Zalalutdinov, K. L. Aubin, R. Rand, B. Houston, J. M. Parpia, and H. G. Craighead, J. Microelectromech. Syst. **14**, 1244 (2005).
- <sup>3</sup>B. Ilic, H. G. Craighead, S. Krylov, W. Senaratne, C. Ober, and P. Neuzil, J. Appl. Phys. **95**, 3694 (2004).
- <sup>4</sup>K. L. Ekinci, X. M. H. Huang, and M. L. Roukes, Appl. Phys. Lett. **84**, 4469 (2004).
- <sup>5</sup>M. D. LaHaye, O. Buu, B. Camarota, and K. C. Schwab, Science **304**, 74 (2004).
- <sup>6</sup>K. Y. Yasumura, T. D. Stowe, E. M. Chow, T. Pfafman, T. W. Kenny, B. C. Stipe, and D. Rugar, J. Microelectromech. Syst. **9**, 117 (2000).
- <sup>7</sup>D. W. Carr, S. Evoy, L. Sekaric, H. G. Craighead, and J. M. Parpia, Appl. Phys. Lett. **75**, 920 (1999).
- <sup>8</sup>K. L. Ekinci and M. L. Roukes, Rev. Sci. Instrum. **76**, 061101 (2005).
- <sup>9</sup>H. Haucke, X. Liu, J. F. Vignola, B. H. Houston, M. H. Marcus, and J. W. Baldwin, Appl. Phys. Lett. **86**, 181903 (2005).

- <sup>10</sup>K. L. Aubin, M. Zalalutdinov, R. Reichenbach, B. Houston, A. T. Zehnder, J. M. Parpia, and H. G. Craighead, Proc. SPIE **5116**, 531 (2003).
- <sup>11</sup>J. Yang, T. Ono, and M. Esashi, Appl. Phys. Lett. **77**, 3860 (2000).
- <sup>12</sup>Y. Wang, J. A. Henry, S. Debohdonyaa, and M. A. Hines, Appl. Phys. Lett. **85**, 5736 (2004).
- <sup>13</sup>L. Sekaric, D. W. Carr, S. Evoy, J. M. Parpia, and H. G. Craighead, Sens. Actuators, A **101**, 215 (2002).
- <sup>14</sup>X. M. H. Huang, M. K. Prakash, C. A. Zorman, M. Mehregany, and M. L. Roukes, *12th International Conference on Transducers, Solid-State Sensors, Actuators and Microsystems 2003*, Vol. 1, pp. 342–343.
- <sup>15</sup>D. A. Czaplewski, S. S. Verbridge, J. Kameoka, and H. G. Craighead, Nano Lett. **4**, 437 (2004).
- <sup>16</sup>W. Weaver, Jr., S. P. Timoshenko, and D. H. Young, *Vibration Problems in Engineering* (Wiley Interscience, New York, 1990).
- <sup>17</sup>H. O. Pierson, *Handbook of Chemical Vapor Deposition: Principles, Technology, and Applications*, 2nd ed. (William Andrew Publishing, LLC, Norwich, NY, 1999).
- <sup>18</sup>L. Kiesewetter, J. M. Zhang, D. Houdeau, and A. Steckenborn, Sens. Actuators, A **35**, 153 (1992).
- <sup>19</sup>K. Wago, O. Zuger, R. Kendrick, C. S. Yannoni, and D. Rugar, J. Vac. Sci. Technol. B **14**, 1197 (1996).
- <sup>20</sup>X. Liu, J. F. Vignola, H. J. Simpson, B. R. Lemon, B. H. Houston, and D. M. Photiadis, J. Appl. Phys. **97**, 023524 (2005).
- <sup>21</sup>J. Gaspar, V. Chu, and J. P. Conde, Appl. Phys. Lett. **84**, 622 (2004).
- <sup>22</sup>Y. T. Yang, K. L. Ekinci, X. M. H. Huang, L. M. Schiavone, and M. L. Roukes, Appl. Phys. Lett. **78**, 162 (2001).
- <sup>23</sup>L. Sekaric, J. M. Parpia, H. G. Craighead, T. Feygelson, B. H. Houston, and J. E. Butler, Appl. Phys. Lett. **81**, 4455 (2002).
- <sup>24</sup>B. Ilic, S. Krylov, K. Aubin, R. Reichenbach, and H. G. Craighead, Appl. Phys. Lett. **86**, 193114 (2005).
- <sup>25</sup>D. M. Photiadis and J. A. Judge, Appl. Phys. Lett. **85**, 482 (2004).
- <sup>26</sup>D. A. Czaplewski, J. P. Sullivan, T. A. Friedmann, D. W. Carr, B. E. N. Keeler, and J. R. Wendt, J. Appl. Phys. **97**, 023517 (2005).
- <sup>27</sup>B. H. Houston, D. M. Photiadis, M. H. Marcus, J. A. Bucaro, X. Liu, and J. F. Vignola, Appl. Phys. Lett. **80**, 1300 (2002).
- <sup>28</sup>R. Lifshitz and M. L. Roukes, Phys. Rev. B **61**, 5600 (2000).
- <sup>29</sup>W. H. Chuang, T. Luger, R. K. Fettig, and R. Ghodssi, J. Microelectromech. Syst. **13**, 870 (2004).
- <sup>30</sup>*CRC Materials Science and Engineering Handbook* (CRC, Boca Raton, FL, 1992).
- <sup>31</sup>X. Zhang and C. P. Grigoropoulos, Rev. Sci. Instrum. **66**, 1115 (1995).
- <sup>32</sup>A. Husain, J. Hone, H. W. Ch. Postma, X. M. H. Huang, T. Drake, M. Barbic, A. Scherer, and M. L. Roukes, Appl. Phys. Lett. **83**, 1240 (2003).
- <sup>33</sup>K. L. Ekinci, Y. T. Yang, X. M. H. Huang, and M. L. Roukes, Appl. Phys. Lett. **81**, 2253 (2002).
- <sup>34</sup>X. Li, T. Ono, Y. Wang, and M. Esashi, *The Fifteenth IEEE International Conference on Micro Electro Mechanical Systems*, 2002, pp. 427–430.